Magnon and soliton excitations in the carrier-poor, one-dimensional S=1/2 antiferromagnet Yb4As3

F. Steglich, M. Köppen, Philipp Gegenwart, T. Cichorek, B. Wand, M. Lang, P. Thalmeier, B. Schmidt, H. Aoki, A. Ochiai

Angaben zur Veröffentlichung / Publication details:

Steglich, F., M. Köppen, Philipp Gegenwart, T. Cichorek, B. Wand, M. Lang, P. Thalmeier, B. Schmidt, H. Aoki, and A. Ochiai. 2000. "Magnon and soliton excitations in the carrier-poor, one-dimensional S=1/2 antiferromagnet Yb4As3." *Acta Physica Polonica A* 97 (1): 91–100. https://doi.org/10.12693/aphyspola.97.91.

Proceedings of the European Conference "Physics of Magnetism '99", Poznań 1999

MAGNON AND SOLITON EXCITATIONS IN THE CARRIER-POOR, ONE-DIMENSIONAL $S = 1/2$ ANTIFERROMAGNET Yb_4As_3

F. STEGLICH, M. KÖPPEN, P. GEGENWART, T. CICHOREK, B. WAND, M. LANG, P. THALMEIER, B. SCHMIDT

Max-Planck Institute for Chemical Physics of Solids, 01187 Dresden, Germany

H. AOKI AND A. OCHIAI

Department of Material Science and Technology, Niigata 950-21, Japan

The semimetallic quasi-one-dimensional $S = 1/2$ Heisenberg antiferromagnet Yb_4As_3 was studied by low-temperature measurements of the specific heat $C(T, B)$, thermal expansion $\alpha(T, B)$, and thermal conductivity $\kappa(T, B)$. At finite magnetic fields ($B \leq 12$ T) we observed the following distinct anomalies: (1) the magnon contribution to $C(T, 0)$, γT, with large coefficient $\gamma \approx 200$ mJ/(K^2 mol), becomes strongly reduced with field, and (2) a broad hump in $C(T, B = \text{const})$ is induced at slightly higher temperatures. (3) The latter corresponds to a pronounced peak in $\alpha(T, B = \text{const})$ as well as (4) to a broad minimum in $\kappa(T, B = \text{const})/\kappa(\text{T}, 0)$. These anomalies are well described by the classical sine-Gordon solution of a one-dimensional Heisenberg antiferromagnet with a weak easy-plane anisotropy. However, the soliton-rest energy deduced from the experimental results depends on the magnetic field like $E_S \sim B^\nu$, with an exponent $\nu \approx 0.66$, while the classical sine-Gordon model requires $\nu = 1$. Thus, our results suggest an alternative description of soliton excitations in an antiferromagnetic $S = 1/2$ Heisenberg chain in terms of the quantum sine-Gordon model, for which an exponent $\nu = 2/3$ is appropriate.

PACS numbers: 75.30.Mb, 65.50.+m, 65.70.+y

1. Introduction

Quasi-one-dimensional magnets continue to attract the attention of theorists and experimentalists. Recent interest has been focussing on antiferromagnetic (AF) quantum-spin-chain systems. For the organic compound copper benzoate $[Cu(C_6D_5COO)_2 \cdot 3D_2O]$, the low-energy excitations in a magnetic field transverse to the Cu^{2+}-chain direction have been identified, via neutron-scattering measurements, as soft modes at incommensurate wave vectors in the vicinity of the AF

wave vector [1]. In addition, low-temperature specific-heat experiments done on this system reveal a magnon-derived linear in-T dependence in the absence of a magnetic field. At a finite field, a gap is found to open in the magnon-excitation spectrum, the size of which depends on both the magnitude and the orientation of the field with respect to the spin chains [1]. This result was explained within the frame of the quantum sine-Gordon (SG) theory, taking into account a staggered field perpendicular to the chains [2].

The inorganic compound Yb_4As_3 also contains AF quantum-spin chains. However, these are not present from the outset but form as a result of a charge--ordering transition near room temperature [3]: at high temperature, Yb_4As_3 is a homogeneous intermediate-valent (IV) metal, for which charge balance dictates a valence ratio of $Yb^{2+} : Yb^{3+} = 3 : 1$. The Yb ions are residing on the four interpenetrating families of cubic space diagonals. At $T_{co} = 292$ K, a first-order phase transition takes place into a mixed-valent state, in which the Yb^{3+} and Yb^{2+} ions spatially order. Since the nearest-neighbor distance between Yb ions residing on different cubic space diagonals is smaller than that within the same chain, minimization of the Coulomb repulsion between the holes on the local $4f$ shell below T_{co} requires that the Yb^{3+} ions are occupying one family of parallel $\langle 111 \rangle$ chains, while the nonmagnetic divalent Yb ions (with their full $4f^{14}$ shell) reside on the other three families of cubic space diagonals. Because of the smaller ionic size of Yb^{3+} compared to Yb^{2+}, the charge ordering goes along with a shrinkage of the $\langle 111 \rangle$ axis, i.e., with a first-order transition from the anti-Th_3P_4 structure (space group $I43d$) to a trigonal one with $\alpha = 90.8°$ (space group $R3c$). The cubic symmetry of the high-T phase of Yb_4As_3 with four equivalent $\langle 111 \rangle$ space diagonals gives rise to a multidomain structure in the charge-ordered trigonal state. As shown in [3], a monodomain crystal can be obtained if a uniaxial pressure of ≈ 80 bar is applied parallel to one of the four cubic space diagonals prior to cooling through T_{co}. Inelastic neutron-scattering experiments performed in the low-temperature trigonal phase, reveal a crystal-field (CF) splitting of the $J = 7/2$ state of the Yb^{3+} ions into four Kramers doublets [4]. The excitation energy of the lowest excited doublet amounts to 14 meV. At temperatures $T < 20$ K one can, therefore, consider almost all of the Yb^{3+} ions to be in their CF ground-state doublet, i.e., in an effective $S = 1/2$ state.

The low-energy excitations of the Yb^{3+} chains have been found, again through inelastic neutron-scattering experiments [4], to agree well with the des Cloizeaux–Pearson spectrum (two-spinon continuum) of an AF $S = 1/2$ chain. Its linear dispersion, both at the center and boundary of the AF Brillouin zone, is connected with the coefficient γ of $C_{sw} = \gamma T$, the spin-wave (more precisely spinon) contribution to the low-T specific-heat via $\gamma = (2/3)|J|^{-1}$. According to the neutron-scattering results [4], $J \approx -k_B \times 25$ K, which is in good agreement with $\gamma \approx 200$ mJ/(K^{2}mol) [5–7].

Yb_4As_3 is semimetallic in the charge-ordered regime with a carrier density of $\approx 10^{-3}$ As-4p holes per formula unit [3]. The low-T (4 K $< T < 20$ K) resistivity behaves as $\rho = \rho_0 + aT^2$ (ρ_0 being the residual resistivity) with a huge coefficient a. For one sample, a was found [3] to scale with γ^2 like in the heavy-fermion metals, which led early workers in this field to call Yb_4As_3 a "heavy-fermion sys-

tem with extremely low carrier concentration". We do not wish to address here the semimetallic behavior of Yb_4As_3 which is discussed, e.g., in [8, 9]. *Despite* the presence of a small number of charge carriers we consider the charge-ordered variant of Yb_4As_3 a model system for studying the low-lying excitations of AF $S = 1/2$ chains, both at $B = 0$ and at finite fields. To this purpose, we discuss in the following sections results of the specific-heat, thermal expansion, and thermal conductivity. While the former results are new, the latter ones have already been published in [10]. We shall compare our data with those reported for Cu benzoate [1] and put them into perspective in the concluding section. The experiments were performed with Yb_4As_3 single crystals grown as described in [3]. For the new specific-heat experiments a commercial "microcalorimeter" (Oxford Instruments) was utilized.

2. Specific heat

In Fig. 1 we show specific-heat data, as C/T vs. T, obtained between 1.5 and 10 K at $B = 0$ and fields up to 12 T for an Yb_4As_3 single crystal. The magnetic field was applied perpendicular to the $\langle 111 \rangle$ direction, which coincides with the short $S = 1/2$ chains for a certain (unknown) volume fraction of this multidomain sample. The low-T data at zero field confirm the linear temperature dependence of the specific heat, γT, with $\gamma \approx 200$ mJ/(K^2 mol), already known from previous work [5–7]. Two distinct observations are made in finite fields: firstly, the low-T specific-heat coefficient $\gamma(T) = C(T)/T$ becomes suppressed, and secondly, a broad hump develops at somewhat higher temperatures. Upon increasing field,

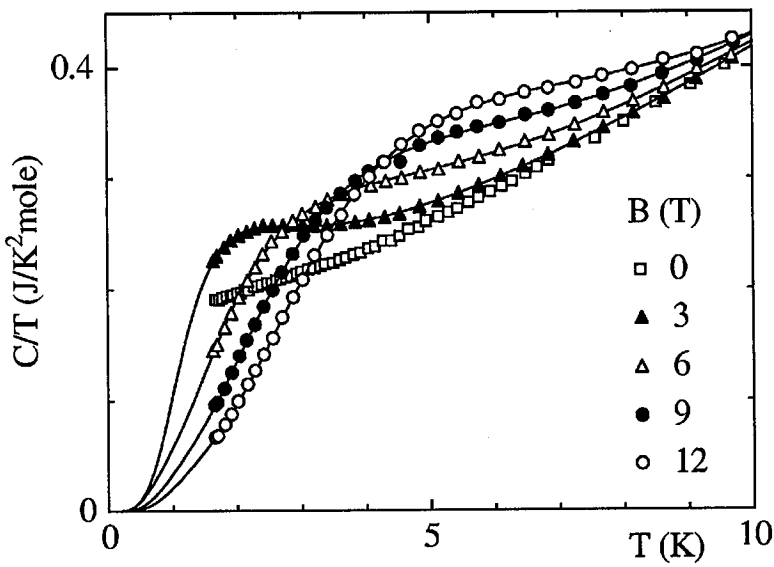

Fig. 1. Specific heat of an Yb_4As_3 single crystal with unknown multidomain structure at $B = 0$ and differing finite fields, applied perpendicular to $\langle 111 \rangle$. Solid lines are fits of Eqs. (1)–(4) to the data.

this anomaly in $C(T)/T$ grows in size and shifts toward higher temperatures. Not shown in Fig. 1, a huge upturn in $C(T)/T$, of unknown origin, develops below $T \approx 0.2$ K [7, 10].

As noted before, the in-T linear term that dominates the low-temperature specific heat at $B = 0$ was identified [11] with the AF spin-wave contribution, $C_{sw}(T)$. The suppression of $C_{sw}(T)$ in a finite magnetic field has been related to the field-induced opening of a gap in the magnon spectrum. This was ascribed to a very weak coupling between the $S = 1/2$ chains [12]. As mentioned in the introduction, very similar observations were made for Cu benzoate [1], and a staggered field perpendicular to the $S = 1/2$ chains was proposed [2] as the driving force for the gap opening in this case. Both an alternating g tensor and the Dzyaloshinskii–Moriya interaction may produce this staggered field [2]. If in the case of Yb_4As_3 one takes into account the presence of the As atoms, one finds that (i) the g tensor is alternating along the $\langle 111 \rangle$ direction and (ii) an inversion-symmetry center between two adjacent Yb^{3+} ions is lacking, prerequisite for the Dzyaloshinskii–Moriya interaction to operate. The staggered-field mechanism may, thus, also be relevant and explain the field-induced gap in Yb_4As_3 as proposed in [13], employing the quantum SG model [14, 15]. The latter, however, has the disadvantage of being a low-energy and low-temperature model. Therefore, it describes well the low-T exponential tail of $C_{spin}(T)$, the spin part of the specific heat, but its validity in the most interesting experimental range of the field-induced hump in $C(T)/T$, of the corresponding maximum in the thermal expansion and of the minimum in the thermal conductivity, to be discussed in the following section, has yet to be shown. The same holds true for the crossover to a nearly constant $C_{spin}(T)/T$ well below $T = |J|/k_B$, as suggested by the data on both Cu benzoate, with $|J|/k_B \approx 18$ K (inset of Fig. 4 in [1]), and Yb_4As_3 (Fig. 2a in [10]).

In order to analyze not only the results for the specific heat, but also those for the thermal expansion as well as the thermal conductivity, not addressed in [14, 15], we have to use the classical model, including both magnons and solitons [16], for AF spin chains along z, a weak easy-plane xxz anisotropy and an applied (symmetry-breaking) field in x direction. Following [10], we consider the temperature range $T \lesssim E_s(B)/k_B$, $E_s(B)$ being the soliton-rest energy. For these temperatures, the soliton density per site, $n_s(T)$, is sufficiently low. Then, the measured specific heat can be expressed as

$$C(T) = C_{spin}(T) + C_{ph}(T) = C_{sw}(T) + C_s(T) + C_{ph}(T), \tag{1}$$

where we include an exponential term in the spin-wave contribution in order to account for the field-induced gap, $\delta(B)$, in the magnon spectrum related to a weak interchain coupling [12]:

$$C_{sw}(T) = \gamma T \exp[-\delta(B)/k_B T]. \tag{2}$$

For the soliton contribution, we write [10]

$$C_s(T) = n_s(T)[(E_s/k_B T)^2 - E_s/k_B T - 1/4], \tag{3}$$

while

$$C_{ph}(T) \approx \beta T^3.$$

The solid lines in Fig. 1 show that Eqs. (1)–(4) can well describe our finite-magnetic-field data.

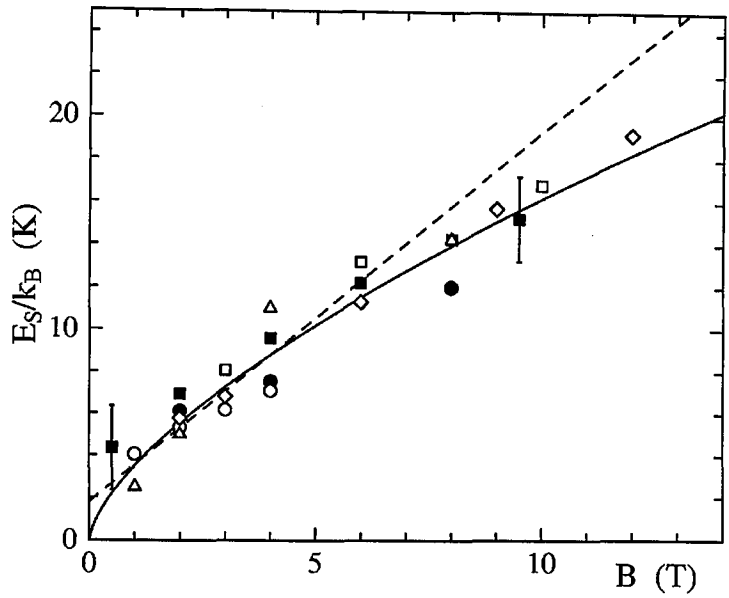

Fig. 2. Soliton-rest energy E_s, divided by k_B, as a function of magnetic field. E_s values are derived from the fits in Figs. 1 (open diamonds), 3 (filled squares), and 4 (open triangles) as well as the rest of data are taken from [10]. Solid line is a fit of $E_s(B) \sim B^{2/3}$ to the data in the whole field range. Dashed straight line is a fit to the low-field data.

The soliton-rest energy derived from these fits of the specific-heat results is shown as a function of the magnetic field in Fig. 2. Here, also $E_s(B)$ values are included as obtained from the thermal-expansion and thermal-conductivity results which we want to discuss in the subsequent section.

We wish to note that the separation of $C_{spin}(T)$ into a spin-wave and a soliton part as given in Eq. (1) is a consequence of our classical approach [16]. This implies that the sizes of the spin-wave gap and the soliton-rest energy are not necessarily the same. In the quantum SG theory, there is no obvious way for this separation, and the most natural assumption is that these two energies are identical [14].

3. Thermal expansion and thermal conductivity

In our thermal-expansion experiment we can apply weak uniaxial pressures between 1 bar and 10 bars along the measuring direction. Thus, the domain--structure configuration of the samples can be deliberately varied. By comparing the observed relative length changes at T_{co}, $\Delta L/L$, with changes of the unit-cell length and angle as determined from X-ray scattering [17], we can estimate the relative volume fraction, x, of the sample in which the $S = 1/2$ chains are oriented parallel to the measuring direction. The remaining volume fraction, $1 - x$, contains domains in which these spin chains run parallel to the other three space diagonals, forming an angle of $\approx 70°$ with respect to the measuring direction. The thermal-expansion data presented in Fig. 3 were taken for an Yb_4As_3 single crystal with $x = 0.35$.

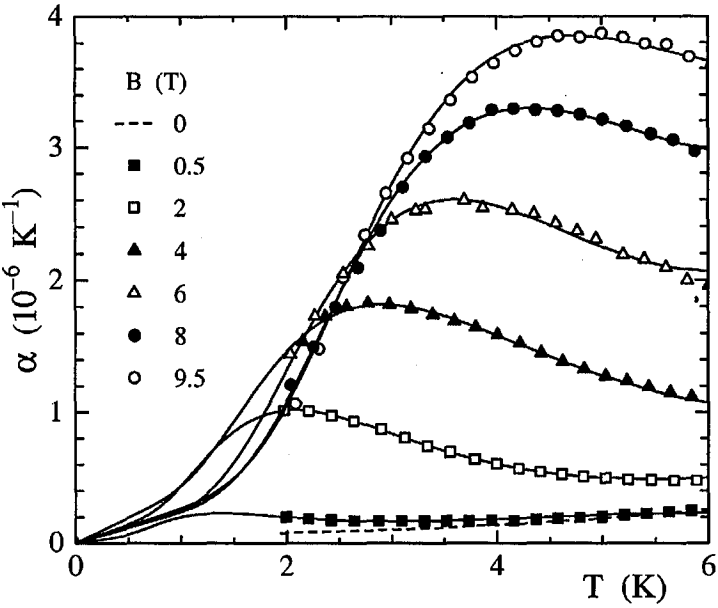

Fig. 3. Coefficient of the thermal expansion, as α vs. T, of an Yb_4As_3 sample with $x = 0.35$ (cf. text) at $B = 0$ and differing magnetic fields. Solid curves represent fits according to Eq. (8).

A quantitative analysis of our thermal-expansion experiments, in which the magnetic field was always applied parallel to the measuring direction, reveals an interesting correlation between the size of the $\alpha(T)$ anomaly, $\alpha_{\max}$, and the actual domain configuration: upon increasing x, $\alpha_{\max}$ becomes reduced in a monotonous fashion and extrapolates to $\alpha_{\max} = 0$ for $x = 1$. Since in this latter case one is dealing with a monodomain structure for which the B field is aligned parallel to the $S = 1/2$ chains, we conclude: the observed anomaly in $\alpha(T, B)$ necessarily requires a finite-field component perpendicular to these chains. We note that, for $\alpha(T)$ measured at zero field, there is a distinct anisotropy with respect to the $\langle 111 \rangle$ direction of the spin chains: $\alpha_{\langle 111 \rangle} < 0$, but $\alpha_{\perp \langle 111 \rangle} > 0$ [10].

Since the orientational dependence of the field-induced anomalies in the thermal expansion cannot be explained either by the extended magnon excitations or by the Schottky contributions, e.g., due to isolated magnetic moments, these anomalies were ascribed in [10] to localized soliton excitations. This appears natural, because like the observed $\alpha(T, B)$ anomalies, the existence of solitons requires a field component perpendicular to the spin chains.

The interpretation of the $\alpha(T, B)$ data, however, is less straightforward than for the $C(T, B)$ data. The soliton contribution $\alpha_s(T, B)$ depends strongly on directional-dependent effects: for example, a quantitative analysis would require the knowledge of the tensor of compliances which is presently not available. To describe only the temperature dependence (but not the magnitude) of $\alpha_s(T, B)$, which is the predominant contribution to the measured thermal expansion, we define (for a fixed B field)

$$\alpha_s(T) = (1/3)\beta_s(T), \tag{5}$$

where β_s is the volume expansion. Then, starting from the Maxwell relation

$$(\partial V/\partial T)_p = -(\partial S_s/\partial p)_T, \tag{6}$$

we obtain

$$\alpha_s = (3V_c c_B)^{-1}\partial S_s/\partial \varepsilon_v, \tag{7}$$

where $S_s = (E_s/k_B T + 1/2)n_s$ is the soliton entropy, $\varepsilon_v = \Delta V/V$ the volume strain, c_B the bulk modulus and V_c the volume per Yb atom. This leads [10] to

$$\alpha_s = [n_s \Gamma/(3V_c c_B)][(E_s/k_B T - 1)^2 - 7/4], \tag{8}$$

where the Grüneisen parameter $\Gamma = {E_s}^{-1}(\partial E_s/\partial \varepsilon_v)$ is much larger than the one due to exchange striction, $\Gamma_{ex} = -J^{-1}(\partial J/\partial \varepsilon_v)$ [10]. In Fig. 3 we show that our $\alpha(T, B)$ results can be described very well by Eq. (8). Note that, compared to the specific-heat analysis, an additional adjustable parameter (Γ) is needed. As for the two remaining fit parameters, i.e., the soliton mass and the soliton-rest energy, we achieve good agreement between these different experimental techniques, cf. [18] and Fig. 2.

We now turn to a brief discussion of our thermal-conductivity results which lend additional support to the existence of magnetic solitons in Yb_4As_3. At $B = 0$ and $T \leq 6$ K, $\kappa_0(T)$ is well represented by [10]

$$\kappa_0(T) = a_1 T + a_2 T^2. \tag{9}$$

The linear term is very likely due to the 1D magnon excitations while the quadratic term is ascribed to the 3D phonons dominantly scattered off the 1D magnons.

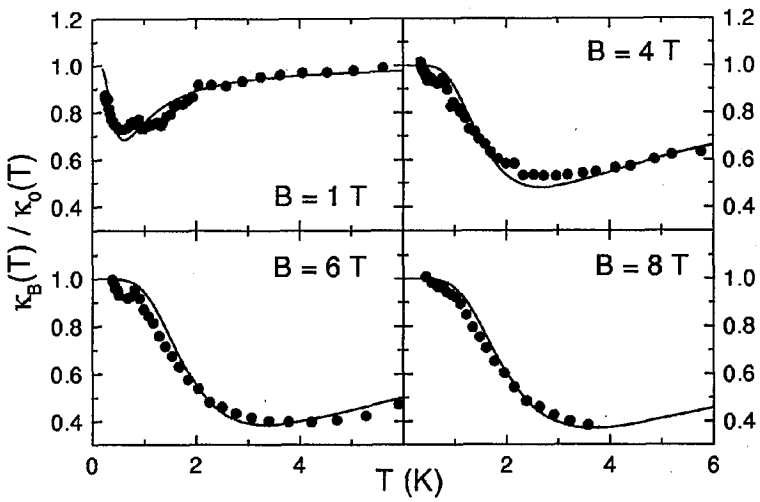

Fig. 4. Thermal conductivity of an Yb_4As_3 sample with (unknown) multidomain structure as a function of temperature for differing magnetic fields. Solid lines are fits for a resonant-phonon-soliton scattering mechanism in the presence of phonon-boundary scattering, as explained in the text.

The low concentration of As-4p holes may also contribute to some extent both to the heat transport and to the phonon scattering. In Fig. 4 we show the thermal conductivity κ_B as a function of temperature for four different magnetic fields between 1 T and 8 T, normalized to $\kappa_0(T)$. In these data, we find a flat minimum which becomes progressively deeper and shifted toward higher temperatures, when we increase the magnetic field. The positions of these minima agree well with those of the $C(T,B)$ and $\alpha(T,B)$ maxima shown in Figs. 1 and 3. We have, therefore, attributed the minima in κ_B/κ_0 vs. T to the scattering of the 3D phonons by the magnetic solitons. This scattering process was already held responsible previously [19] for similar observations in the $S = 5/2$ spin-chain systems TMMC and DMMC: here, a phonon–soliton resonance scattering was assumed, acting independently from the usual phonon-boundary scattering. As fit parameters, the soliton-rest energy and the relative strength of the resonance-scattering mechanism were used. Following [19], we can fit the experimental data of Fig. 4 reasonably well. The field dependence of $E_s(B)$ deduced from the thermal conductivity agrees satisfactorily with $E_s(B)$ derived from both $C(T,B)$ and $\alpha(T,B)$, see Fig. 2.

4. Conclusion

The seeming heavy-fermion behavior of Yb_4As_3, as highlighted by the large specific-heat coefficient $\gamma \approx 200$ mJ/(K^2 mol), was ascribed [11] to the formation of $S = 1/2$ AF Heisenberg chains well below its charge-ordering transition temperature, $T_{co} \approx 292$ K. On the other hand, the 1D AF Heisenberg model cannot explain the strong field dependence of the low-temperature specific heat [5–7]. Interchain coupling [12] and, alternatively, small corrections to the Heisenberg exchange [13] or intrachain dipolar interactions [13] have been proposed as possible reasons of this behavior. Our results for the specific heat, thermal expansion, and thermal conductivity clearly indicate that in the quantum-spin chains of charge-ordered Yb_4As_3, excitations of solitonic nature are present which lead to peaks in the spin contributions to $C(T)$ and especially to $\alpha(T)$ as well as to minima in $\kappa_B(T)/\kappa_0(T)$. An anomaly at $B = 3.5$ T is clearly visible also in the $C(T)/T$ data for Cu benzoate [1], strikingly similar to the soliton peak in the specific-heat data of Fig. 1. For our results on Yb_4As_3, a classical analysis based on the SG model was employed. In this model, the soliton-rest energy is due to the destruction of uniaxial symmetry around $B \parallel x$ (z: chain direction) by an xxz exchange anisotropy and is simply given by $E_s(B) = g_e\mu_B BS$. However, as can be seen in Fig. 2, a fit of the classical SG model to the results of the three different kinds of experiments reveals a field dependence of the soliton-rest energy that disagrees with $E_s \sim B$. This is not surprising, since it has been known already that quantum corrections to the classical SG theory [21] lead to a deviation from the proportionality between E_s and B. As is shown by the solid curve in Fig. 2, a power-law dependence $E_s \sim B^\nu$ with an exponent $\nu = 2/3$ fits the results much better.

Such exponents are known to appear in the quantum version of the SG theory, which is obtained as the effective low-energy form of the $S = 1/2$ AF Heisenberg model by mapping to spinless fermions and subsequent bosonization [2]. The low-energy excitations of the genuine AF Heisenberg model are then described by the effective Lagrangian of a massless scalar field. A finite mass, or excitation

gap, may be introduced by various deviations from the AF Heisenberg model like xxz-exchange anisotropy, dimerization by lattice distortion or staggered fields induced by Dzyaloshinskii–Moriya interaction or alternating g tensors. While the former and the latter of these mechanisms were suggested as being important for the $C(T, B)$ behavior in Cu benzoate [15], the staggered field was, as pointed out before, held responsible for the gap-opening effect in Yb_4As_3 [13]. We still think that the existence of solitons in Yb_4As_3 could possibly be due to the xxz anisotropy as considered in our classical approach. Note that, unlike in Cu benzoate, there is no a priori reason why this anisotropy should be small, since the orbital moments are not quenched in the effective $S = 1/2$ Kramers ground-state doublet of the Yb^{3+} ions.

In conclusion, it would be highly desirable to have finite-temperature density--matrix renormalization-group calculations for the AF xxz model in a transverse field (along x), a problem that cannot presently be solved analytically. So far, only quantum Monte Carlo calculations for the *ferromagnetic* $S = 1/2$ xxz model have been performed [22] which indeed reveal the evolution of a soliton peak as a function of the magnetic field.

Acknowledgments

We should like to thank P. Fulde, M. Kohgi, G. Sawatzki, O. Trovarelli, and especially K. Ueda for valuable conversations and helpful comments.

References

[1] D.C. Dender, P.R. Hammar, D.N. Reich, C. Broholm, G. Aeppli, *Phys. Rev. Lett.* **79,** 1750 (1997).

[2] M. Oshikawa, I. Affleck, *Phys. Rev. Lett.* **79,** 2883 (1997).

[3] A. Ochiai, T. Suzuki, T. Kasuya, *J. Phys. Soc. Jpn.* **59,** 4129 (1990).

[4] M. Kohgi, K. Iwasa, J.-M. Mignot, A. Ochiai, T. Suzuki, *Phys. Rev. B* **56,** R11388 (1997).

[5] O. Nakamura, N. Tomonaga, A. Ochiai, T. Suzuki, T. Kasuya, *Physica B* **171,** 377 (1991).

[6] P.H.P. Reinders, U. Ahlheim, K. Fraas, F. Steglich, T. Suzuki, *Physica B* **186-188,** 434 (1993).

[7] R. Helfrich, M. Köppen, M. Lang, F. Steglich, A. Ochiai, *J. Magn. Magn. Mater.* **177-181,** 309 (1998).

[8] V.N. Antonov, A.N. Yaresko, A.Ya. Perlov, P. Thalmeier, P. Fulde, P.M. Openeer, H. Eschrig, *Phys. Rev. B* **58,** 9752 (1998).

[9] T. Kasuya, private communication.

[10] M. Köppen, M. Lang, R. Helfrich, F. Steglich, P. Thalmeier, B. Schmidt, B. Wand, D. Pankert, H. Benner, H. Aoki, A. Ochiai, *Phys. Rev. Lett.* **82,** 4548 (1999).

[11] P. Fulde, B. Schmidt, P. Thalmeier, *Europhys. Lett.* **31,** 323 (1995).

[12] B. Schmidt, P. Thalmeier, P. Fulde, *Europhys. Lett.* **35,** 109 (1996).

[13] M. Oshikawa, K. Ueda, H. Aoki, A. Ochiai, M. Kohgi, private communication.

[14] M. Fowler, X. Zotos, *Phys. Rev. B* **25,** 5806 (1982).

[15] F.H.L. Eßler, preprint available on http://xxx.lanl.gov, cond-mat/9811309.

[16] K.M. Leung, D.W. Hone, D.L. Mills, P.S. Riseborough, S.E. Trullinger, *Phys. Rev. B* **21**, 4017 (1980).

[17] K. Iwasa, M. Kohgi, N. Nakajima, R. Yoshitake, Y. Hisazaki, H. Osumi, K. Tajima, N. Wakabayashi, Y. Haga, A. Ochiai, T. Suzuki, *J. Magn. Magn. Mater.* **177-181**, 393 (1998).

[18] M. Köppen, Ph.D. thesis, TU Darmstadt 1998, unpublished.

[19] J.A.H.M. Buijs, W.J. de Jonge, *J. Phys. C* **15**, 6631 (1982).

[20] Y. Kudasov, G. Uimin, P. Fulde, A. Ovchinnikov, preprint available on http://xxx.lanl.gov, cond-mat/9910196.

[21] M.D. Johnson, N.F. Wright, *Phys. Rev. B* **32**, 5798 (1985).

[21] I. Satija, G. Wysin, A.R. Bishop, *Phys. Rev. B* **31**, 3205 (1985).